

INVESTIGATING THE COMBUSTION BEHAVIOR OF Al/AP COMPOSITES WITH HIGH-SPEED VIDEOGRAPHY

Yujie Wang, George Issac Paul, & Michael R. Zachariah*

University of California, Riverside, California 92521, USA

*Address all correspondence to: Michael R. Zachariah, Department of Chemical and Environmental Engineering, University of California, Riverside, CA 92521, USA, E-mail: mrz@engr.ucr.edu

In this study, we prepare 90 wt % loading composites of aluminum and ammonia perchlorate with equivalence ratios from 0.5 to 2 and study their combustion behavior with high-speed microscopic and macroscopic videography and pyrometry. For all equivalence ratios, microscopic videography reveals the formation of fractal-shaped agglomerates that transform into molten droplets eventually growing into larger droplets before departing the burning surface. Droplet size analysis suggests that droplets of similar sizes evolve from composites with equivalence ratios of 0.5 and 1, while dramatically larger droplets are observed for a composite with an equivalence ratio of 2. Temperature measurement from three-color pyrometry suggests that there is no difference in temperature among the agglomerates/droplets from different equivalence ratios. Burn rates obtained from the macroscopic imaging show that the burn rate of the composites increases as the equivalence ratio increases, although one expects that an equivalence ratio of 2 should have a lower burn rate due to its lower energy density. Analysis of the droplet residence time on the burning surface shows that while the droplets on the burning surface in the case of composites with equivalence ratios of 0.5 and 1 have similar residence times, droplets at an equivalence ratio of 2 have significantly longer residence times on the burning surface, which results in significantly more heat feedback to the unburnt propellant and leads to the unexpected higher burn rate than an equivalence ratio of 1.

KEY WORDS: aluminum, propellant, agglomeration, combustion, imaging, pyrometry, heat feedback

1. INTRODUCTION

Aluminum (Al) particles are widely used in solid propellants as additives to increase specific impulse and enhance combustion stability (Chen et al., 2017). Al nanoparticles offer a higher energy release rate and lower ignition temperature than traditional Al microparticles (Comet et al., 2019; Granier and Pantoya, 2004; Sundaram et al., 2017, 2016). Nevertheless, the nanostructure of Al nanoparticles is typically rapidly lost prior to and during combustion due to reactive sintering and in-combustion agglomeration (Chakraborty and Zachariah, 2014; Galfetti et al., 2007; Melcher et al., 2012). This means that the effective size of Al particles increases during combustion (Emelyanov et al., 2020; Wang et al., 2021b, 2022). This phenomenon can have a significant impact on the combustion performance of the propellant and is the motivation for imaging studies explored in this work.

The Al particle agglomeration in propellants has been widely observed and a variety of diagnostic techniques have been applied to investigate the particle behavior (Ao et al., 2020; Babuk et al., 1999, 2001; Cohen et al., 2022; Jin et al., 2020; Li et al., 2020; Sippel et al., 2014). *Ex situ* techniques using electron microscopes for characterizing the captured particles from combustion are commonly used to study agglomerates (Ao et al., 2020; Li et al., 2020; Sippel et al., 2014; Tu

et al., 2022). Recently, *in situ* high-speed imaging techniques have proven to be particularly useful for probing spatial and temporal combustion dynamics as well as estimating particle temperatures, and quantifying the size and velocity of Al particles (Chen et al., 2017; Marsh et al., 2021; Wang et al., 2020, 2019b, 2023b). Despite these studies, a systematic investigation focusing on characterizing the combustion behavior of Al/AP (ammonium perchlorate) composites with various equivalence ratios using high-speed imaging techniques is still lacking.

In this paper, we prepare freestanding Al/AP composites with 90% loading with different equivalence ratios by 3D printing and investigate their combustion behavior systematically using high-speed (μs) and high-resolution (μm) imaging techniques, which enable direct visualization of Al agglomerates/droplets evolving during combustion process in-operando. The size and residence time of droplets on the burning surface are measured. Temperature of the burning agglomerates/droplets in the reacting zone is estimated with three-color pyrometry. The burn rates of different composites and droplet velocity after departing from the burning surface are obtained from macroscopic imaging.

2. MATERIALS AND METHODS

2.1 Materials

Aluminum nanoparticles (Al NPs, ~ 70 nm, 66 wt % active) were purchased from US Research Nanomaterials, Inc. The active content of these fuels was determined with thermogravimetry and differential scanning calorimetry (TGA–DSC) using a SDT Q600 from TA Instruments. Ammonia perchlorate microparticles (AP MPs, $90 \mu\text{m}$) were obtained from Pyro Chem Source. Ethanol (200 proof) was purchased from Koptec. Dichloromethane (99.9%) was purchased from Fisher Scientific. Polymethyl methacrylate (PMMA) was purchased from Alfa Aesar.

2.2 Preparation of Ink and Direct Ink Writing of 90 wt % Loading Al/AP Composites

A typical ink was prepared by firstly dissolving 10 wt % of PMMA in the mixture of ethanol and dichloromethane (volumetric ratio of 1:1). AP was then added to the solution and the obtained suspension was sonicated for 15 min. Then Al was added, and the obtained suspension was sonicated for 30 min. After sonication the suspension was stirred for ~ 3 h before printing. The amount of Al and AP was determined with the following equation, and different equivalence ratios ($\phi = 0.5, 1, \text{ and } 2$) were considered.



Details about printing can be found in our previous studies (Wang et al., 2019c). Generally, for printing, an ink was extruded through an 18 gauge (1.2 mm inner diameter) nozzle and written on a glass substrate at room temperature. After printing, the films were cut into ~ 2 cm long sticks for studying combustion behaviors.

2.3 Microscopic and Macroscopic Imaging

The details of the microscopic and macroscopic imaging process can be found in our previous publications (Wang et al., 2020). Briefly, the macroscopic imaging was performed with a high-speed camera (Vision Research Phantom Miro M110) and the microscopic imaging was

performed with a high-speed camera (Vision Research Phantom VEO710L) coupled to a long working length objective (Infinity Photo-Optical Model K2 DistaMax). For a typical measurement, a printed stick was mounted on a stage holder within a chamber filled with argon, and the chamber was placed between the two imaging systems. The stick was then ignited with a nichrome wire by Joule heating. The combustion process was recorded at a sample rate of 10,000 frames/s with the macroscopic imaging system and 24,000 frames/s (512 × 512 pixels, 1.7 μm/pixel) with the microscopic imaging system. The schematic of the setup is shown in Fig. 1.

Size measurement was performed only on spherical droplets (fractal-shaped agglomerates were not counted). For $\phi = 0.5$ and 1, the residence time of droplets was performed in microimaging videos by tracking the starting time of the emergence of the fractal-shaped agglomerates, to the time when the droplets leave the burning surface. For $\phi = 2$, in addition to the aforementioned tracking method in microimaging videos, the residence time of large droplets was also tracked in macroscopic imaging videos due to their much larger size and longer residence time. Particle velocity in the gas phase was measured by tracking the location of the particles and the corresponding time.

2.4 Three-Color Imaging Pyrometry

Details about three-color imaging pyrometry can be found in the previous studies from our group (Jacob et al., 2018; Wang et al., 2019a). Briefly, temperature estimation of a sample was performed with the ratios of channel intensities of three colors (red, green, blue) from the Bayer filter by using a custom MATLAB routine assuming graybody emission behavior of the sample. Calibration parameters were collected by the response to a blackbody source (Mikron M390) and the temperature uncertainty was estimated to be nominally 200–300 K (Kline et al., 2020; Wang et al., 2021b).

3. RESULTS AND DISCUSSION

High-speed microscopic videos enable direct visualization of events on the burning surface, which provides key understanding of the combustion characteristics. Figure 2 (top) shows the representative snapshots from the high-speed microscopic videos for Al-AP with different equivalence ratios. For all three equivalence ratios, fractal-shaped agglomerates form and transform into molten droplets with dark caps, which may coalesce into larger droplets. Micron-scale Al undergoes vapor phase combustion, via Al vaporization, and condensation and growth of the oxide (Wang et al., 2023b; Emelyanov et al., 2020). The aluminum residing on the surface is in the early stages of combustion, which is obviously true for the agglomerates, but also true for the

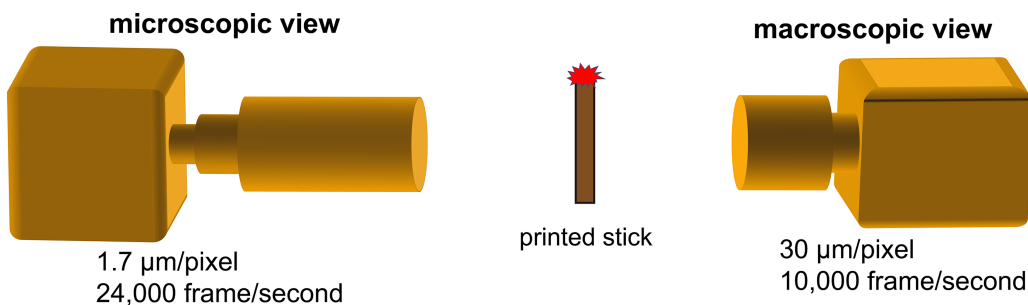


FIG. 1: Setup of the microscopic and macroscopic imaging systems

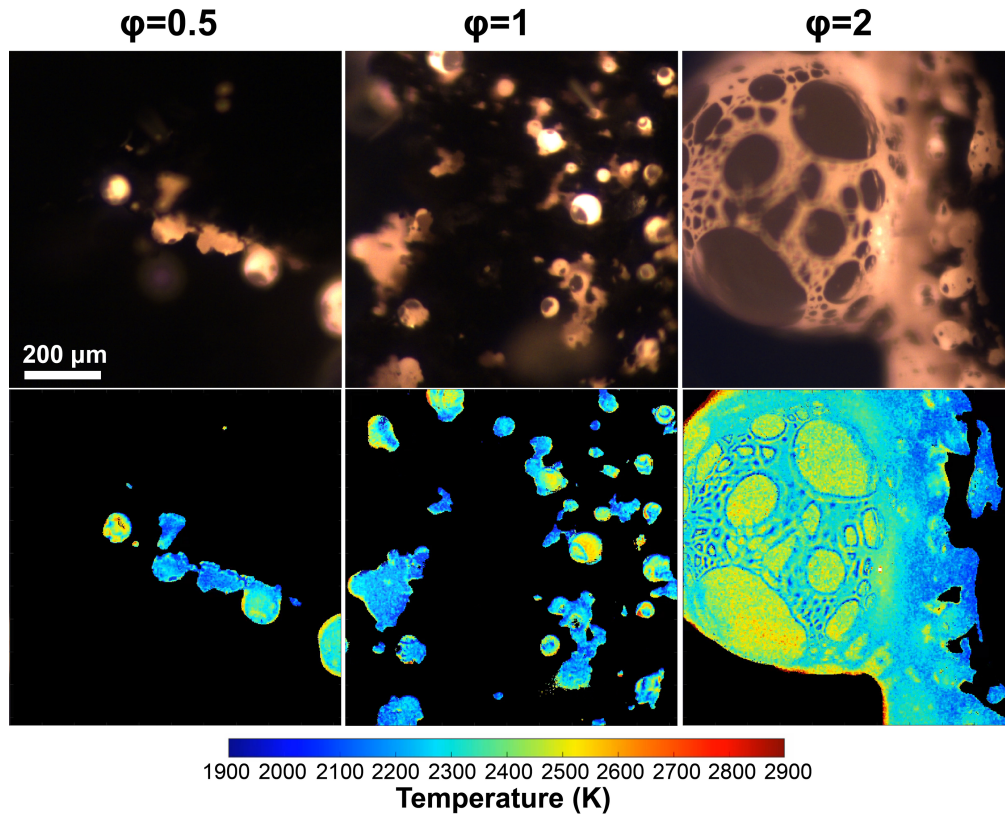


FIG. 2: Representative images from high-speed microscopy video for Al-AP at different equivalence ratios on the top and their corresponding temperature map from three-color pyrometry on the bottom. High-error points and low-intensity points were excluded from the temperature calculation.

droplets, and will be discussed in more detail in the following section when we compare surface residence and combustion times. For equivalence ratios of 0.5 and 1, these droplets depart from the burning surface, and do not significantly coalesce further, while for an equivalence ratio of 2, the majority of droplets merge into much larger droplets before leaving the burning surface. Size distribution of the droplets and its impact on the macroscopic combustion behavior will be discussed further in the following section.

Three-color (RGB) pyrometry was used for estimating the temperature of the agglomerates/droplets and the obtained representative temperature maps for different equivalence ratios are shown in Fig. 2 (bottom). For all three equivalence ratios, fractal-shaped agglomerates have a temperature of ~ 2100 K. Although this temperature is significantly higher than the melting point of Al at 930 K, it is lower than the melting point of Al_2O_3 at 2345 K (Chen et al., 2017); therefore Al_2O_3 is in the solid state and prevents the fractal-shaped agglomerate from becoming droplets. As oxidation continues and temperature increases near the melting point (~ 2345 K), Al_2O_3 melts and phase separates from Al, and retracts into a distinct cap through surface tension (Harrison and Brewster, 2009). The measured temperature of the droplets is ~ 2350 K, which is about the melting point of Al_2O_3 , explaining the observed nearly spherical morphology. It is noteworthy that although droplets of an equivalence ratio of 2 are significantly larger than equivalence ratios of 0.5 and 1, these droplets have about the same temperature at ~ 2350 K. From the thermal map the hot

spots are believed to be the oxide “caps.” For an equivalence of 2, it is clear that the Al_2O_3 cap is slightly hotter (~ 150 K) than the Al body, consistent with the observations from previous studies (Chen et al., 2017; Wang et al., 2023b). However, this exact difference is within the accuracy limits of our diagnostic, but we can say is that the oxide is hotter. This temperature difference can likely be attributed to the evaporation of Al which is endothermic while condensation of alumina is exothermic. Finally, and as will be discussed in the next section, aluminum residing on the surface is in the early stages of combustion implying that alumina is still a minor component.

Size distributions of droplets observed in microimaging videos for Al-AP with different equivalence ratios are displayed in Fig. 3(a). There is minimal difference in size distribution between equivalence ratios of 0.5 and 1, as the majority of the droplets for both equivalence ratios are below $120 \mu\text{m}$. While for an equivalence ratio of 2, the overall droplet sizes are dramatically larger with more than half of the droplets being above $200 \mu\text{m}$. It is noteworthy that the size of the primary Al particles initially incorporated into the composite is 70 nm , which implies that there is extensive sintering/coalescence and agglomeration of Al during the combustion process and the sintering/agglomeration extent of an equivalence of 2 is significantly higher, as the size

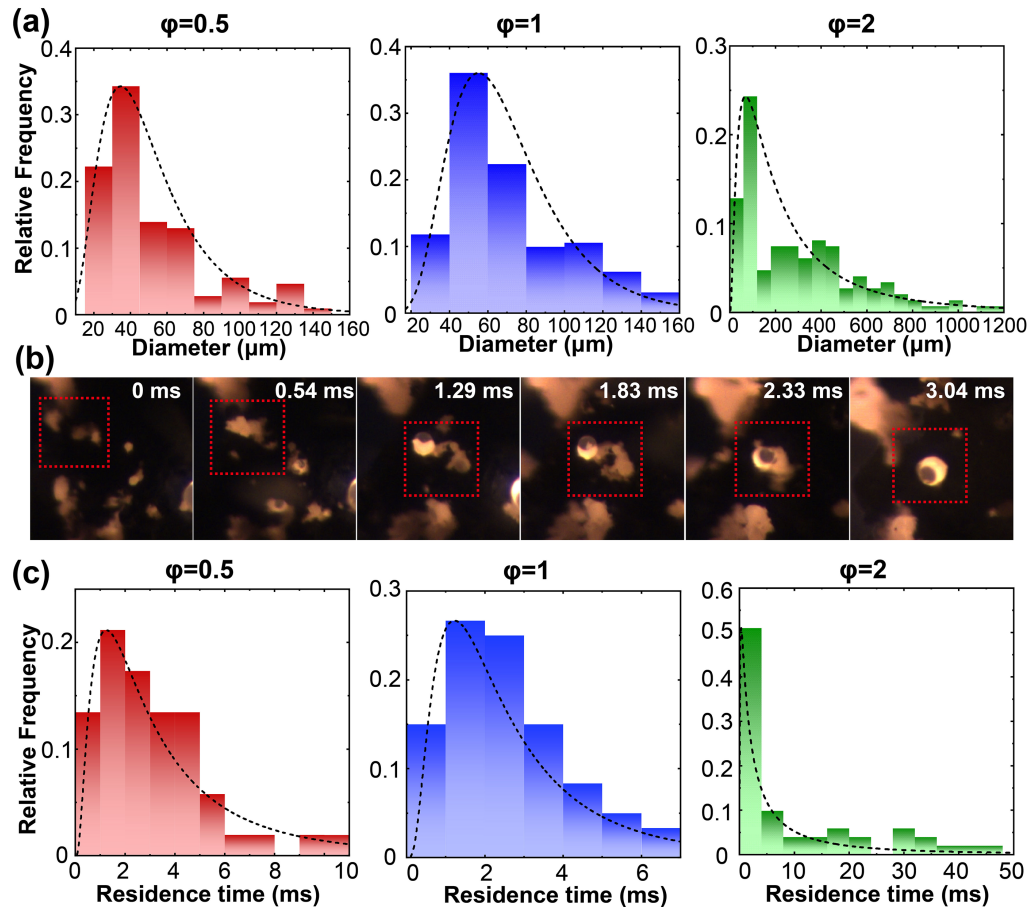


FIG. 3: Droplet size distribution of Al-AP with different equivalence ratios (a), time-resolved snapshots of a representative droplet evolving before departing from the burning surface for $\phi = 1$ (b), and residence time distribution of Al-AP with different equivalence ratios (c)

increases ~ 1000 times for equivalence ratios of 0.5 and 1, whereas it increases ~ 4500 times in the case of an equivalence ratio of 2.

Figure 3(b) displays a series of snapshots of a representative droplet forming from a fractal-shaped agglomerate and growing before departing from the burning surface at an equivalence ratio of 1. This visualization shows that the droplets burn for some time on the burning surface rather than departing upon formation. The droplet residence time on the burning surface is estimated based on the time span from the emergence of an agglomerate that evolves into a droplet to the departure of that droplet, and the obtained residence time distributions of different equivalence ratios are shown in Fig. 3(c). Similar to the size distribution comparison, there is minimal difference in droplet residence time between equivalence ratios of 0.5 and 1, and the majority of the residence times are less than 6 ms, while for an equivalence ratio of 2, the overall residence time is significantly higher, with about 40% of the droplets having residence times of more than 8 ms. The burn time of Al droplets, estimated based on a droplet evaporation model from our previous study (Wang et al., 2023b), is ~ 50 ms for a $100\ \mu\text{m}$ Al droplet and ~ 1 s for a $500\ \mu\text{m}$ Al droplet. For the composites with equivalence ratios of 0.5 and 1, the droplet surface residence time is generally less than 10% of the estimated burn time. In the case of the composite with an equivalence ratio of 2, the droplet surface residence time is less than 5% of the estimated burn time. These findings suggest that the structures observed on the burning surface are in the early stages of combustion. This is confirmed by their continued burning after detaching from the surface, a phenomenon consistent with the observations from macroscopic imaging. Further details will be discussed in the following section.

Burn rate of a composite normally reflects its energy release rate and provides insight into the overall combustion performance (Wang et al., 2023a, 2019a). Figure 4(a) displays a series

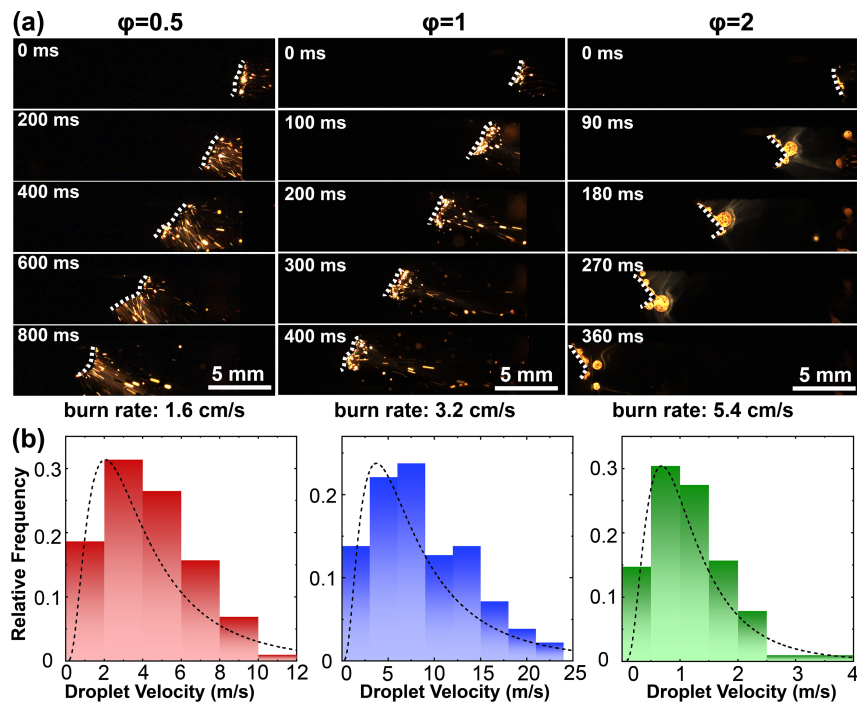


FIG. 4: Time resolved-snapshots of high-speed macroscopic video with corresponding burn rate (a), and droplet velocity distribution (b) of Al-AP with different equivalence ratios. Note: the dashed lines represent burning surfaces.

of time-resolved snapshots from the macroscopic videos for different equivalence ratios, with their corresponding burn rates. It is worth noting that some droplets are sufficiently large to be resolved in the macroscopic videos for an equivalence ratio of 2. The droplets continue burning after departing from the burning surface, and the droplet velocity in the gas phase is measured by tracking the distance and the corresponding time. The obtained velocity distribution is shown in Fig. 4(b), which reveals that the majority of droplets have a velocity above 2 m/s for equivalence ratios of 0.5 and 1, while for an equivalence ratio of 2, the droplet velocity is mostly below 2 m/s. This difference is attributed to the considerably larger droplet size of an equivalence ratio of 2 compared to equivalence ratios of 0.5 and 1. It is interesting that although there is only minimal difference between equivalence ratios of 0.5 and 1 for both droplet size and residence time on the burning surface, the droplet velocity in the gas phase of an equivalence of 1 is about twice that of an equivalence ratio of 0.5. As the equivalence ratios change from 0.5 and 1, the AP content decreases slightly, which means the amount of gas generated cannot explain this difference. Nevertheless, the heat generated from an equivalence ratio of 1 is almost twice that of an equivalence ratio of 0.5. The higher amount of heat generation causes faster gas expansion performing PV work by pushing the droplets apart and thereby results in a higher droplet velocity, which is believed to be the primary reason for a higher droplet velocity of an equivalence ratio of 1.

As the equivalence ratio increases from 0.5 (fuel lean) to 1, the burn rate increases as expected from 1.6 to 3.2 cm/s. As the equivalence ratio increase from 1 to 2 (fuel rich), the burn rate is expected to decrease as the overall energy density of the composite is reduced due to the excess content of fuel, and the burn tests are performed in an argon environment that provides no extra oxygen. However, we observe that the burn rate increases from 3.2 to 5.4 cm/s when the equivalence ratio increases from 1 to 2. Previous studies have demonstrated that reduction in agglomeration/sintering of aluminum particles effectively promotes the propagation rate (Brewster and Hardt, 1991; Sippel et al., 2014; Wang et al., 2022, 2021a,b). A primary question now arises: why does the composite with an equivalence ratio of 2 have a higher burn rate than an equivalence ratio of 1 even though it has lower energy density and significantly more severe sintering/agglomeration?

For propagation, sufficient heat transferred from the flame back to the unreacted material is essential for steady propagation (Brewster and Hardt, 1991; Egan and Zachariah, 2015; Ishihara et al., 1991; Kline et al., 2020). For Al-based composites, previous studies have demonstrated through calculation that conduction is not the dominant source for heat feedback to the unburnt material (Egan and Zachariah, 2015; Kline et al., 2020). These calculations had the underlying assumption that burning particles depart from the burning surface immediately after reaching a certain temperature. However, in the case of the current study, droplets reside on the burning surface for a significant duration after reaching the maximum temperature. Figure 2 shows that droplets from composites with different equivalence ratios have the same temperature, which suggests a higher amount of absolute energy has been provided as conductive heat feedback for a longer residence time, assuming other factors remain invariant. As discussed above, the droplet residence time from a composite with an equivalence ratio of 2 is significantly longer than an equivalence ratio of 1, which indicates that a higher amount of total heat is provided back to the unburnt material from the burning droplets for an equivalence ratio of 2 than an equivalence ratio of 1. This higher heat feedback results in an enhanced burn rate, and this enhancement exceeds the reduction effects from lower energy density, and more severe sintering/agglomeration. Therefore, a higher burn rate is observed for the composite with an equivalence ratio of 2 than an equivalence ratio of 1.

4. CONCLUSION

In this study, high-speed microscopic and macroscopic imaging techniques were used as the primary diagnostic tools for investigating the combustion behavior of 3D printed 90% loading

Al-AP propellants with different equivalence ratios ($\phi = 0.5, 1, \text{ and } 2$) in an inert environment. Microscopic imaging shows that for all three equivalence ratios, fractal-shaped agglomerates transition into spherical droplets that grow into larger droplets before departing the burning surface. While droplets with similar sizes are observed for equivalence ratios 0.5 and 1, significantly larger droplets form for an equivalence ratio of 2. Three-color pyrometry employed for measuring agglomerate/droplet temperature shows there is no difference among the agglomerates/droplets from different equivalence ratios. Macroscopic imaging reveals that the burn rate of the composite increases as the equivalence ratio increases. Residence time analysis shows a droplet evolving from a composite with an equivalence ratio of 2 has a dramatically longer residence time on the burning surface than equivalence ratios of 0.5 and 1. This significantly longer residence time is believed to result in more heat feedback to the unburnt composite which causes the unexpected higher burn rate than an equivalence ratio of 1. This study reveals the dominance of conductive heat feedback on the propagation rate of an aluminized propellant.

ACKNOWLEDGMENT

This work was supported by AFOSR.

REFERENCES

- Ao, W., Liu, P., Liu, H., Wu, S., Tao, B., Huang, X., and Li, L.K.B., Tuning the Agglomeration and Combustion Characteristics of Aluminized Propellants via a New Functionalized Fluoropolymer, *Chem. Eng. J.*, vol. **382**, p. 122987, 2020.
- Babuk, V.A., Vasilyev, V.A., and Malakhov, M.S., Condensed Combustion Products at the Burning Surface of Aluminized Solid Propellant, *J. Propuls. Power*, vol. **15**, no. 6, pp. 783–793, 1999.
- Babuk, V.A., Vasilyev, V.A., and Sviridov, V.V., Propellant Formulation Factors and Metal Agglomeration in Combustion of Aluminized Solid Rocket Propellant, *Combust. Sci. Technol.*, vol. **163**, no. 1, pp. 261–289, 2001.
- Brewster, M.Q. and Hardt, B.E., Influence of Metal Agglomeration and Heat Feedback on Composite Propellant Burning Rate, *J. Propuls. Power*, vol. **7**, no. 6, pp. 1076–1078, 1991.
- Chakraborty, P. and Zachariah, M.R., Do Nanoenergetic Particles Remain Nano-Sized during Combustion? *Combust. Flame*, vol. **161**, no. 5, pp. 1408–1416, 2014.
- Chen, Y., Guildenbecher, D.R., Hoffmeister, K.N.G., Cooper, M.A., Stauffacher, H.L., Oliver, M.S., and Washburn, E.B., Study of Aluminum Particle Combustion in Solid Propellant Plumes Using Digital In-Line Holography and Imaging Pyrometry, *Combust. Flame*, vol. **182**, pp. 225–237, 2017.
- Cohen, O., Michaels, D., and Yavor, Y., Agglomeration in Composite Propellants Containing Different Nano-Aluminum Powders, *Propellants, Explos., Pyrotech.*, vol. **47**, no. 9, 2022.
- Comet, M., Martin, C., Schnell, F., and Spitzer, D., Nanothermites: A Short Review. Factsheet for Experimenters, Present and Future Challenges, *Propellants, Explos., Pyrotech.*, vol. **44**, no. 1, pp. 18–36, 2019.
- Egan, G.C. and Zachariah, M.R., Commentary on the Heat Transfer Mechanisms Controlling Propagation in Nanothermites, *Combust. Flame*, vol. **162**, no. 7, pp. 2959–2961, 2015.
- Emelyanov, V.N., Teterina, I.V., and Volkov, K.N., Dynamics and Combustion of Single Aluminium Agglomerate in Solid Propellant Environment, *Acta Astronaut.*, vol. **176**, pp. 682–694, 2020.
- Galfetti, L., DeLuca, L.T., Severini, F., Colombo, G., Meda, L., and Marra, G., Pre and Post-Burning Analysis of Nano-Aluminized Solid Rocket Propellants, *Aerosp. Sci. Technol.*, vol. **11**, no. 1, pp. 26–32, 2007.
- Granier, J.J. and Pantoya, M.L., Laser Ignition of Nanocomposite Thermites, *Combust. Flame*, vol. **138**, no. 4, pp. 373–383, 2004.
- Harrison, J. and Brewster, M.Q., Analysis of Thermal Radiation from Burning Aluminium in Solid Propellants, *Combust. Theory Modell.*, vol. **13**, no. 3, pp. 389–411, 2009.

- Ishihara, A., Brewster, M.Q., Sheridan, T.A., and Krier, H., The Influence of Radiative Heat Feedback on Burning Rate in Aluminized Propellants, *Combust. Flame*, vol. **84**, no. 1, pp. 141–153, 1991.
- Jacob, R.J., Kline, D.J., and Zachariah, M.R., High Speed 2-Dimensional Temperature Measurements of Nanothermite Composites: Probing Thermal vs. Gas Generation Effects, *J. Appl. Phys.*, vol. **123**, no. 11, p. 115902, 2018.
- Jin, B., Wang, Z., Xu, G., Ao, W., and Liu, P., Three-Dimensional Spatial Distributions of Agglomerated Particles on and near the Burning Surface of Aluminized Solid Propellant Using Morphological Digital In-Line Holography, *Aerosp. Sci. Technol.*, vol. **106**, p. 106066, 2020.
- Kline, D.J., Alibay, Z., Rehwoldt, M.C., Idrogo-Lam, A., Hamilton, S.G., Biswas, P., Xu, F., and Zachariah, M.R., Experimental Observation of the Heat Transfer Mechanisms that Drive Propagation in Additively Manufactured Energetic Materials, *Combust. Flame*, vol. **215**, pp. 417–424, 2020.
- Li, L., Chen, X., Zhou, C., Li, W., and Zhu, M., Experimental and Model Investigation on Agglomeration of Aluminized Fuel-Rich Propellant in Solid Fuel Ramjet, *Combust. Flame*, vol. **219**, pp. 437–448, 2020.
- Marsh, A.W., Wang, G.T., Heyborne, J.D., Guildenbecher, D.R., and Mazumdar, Y.C., Time-Resolved Size, Velocity, and Temperature Statistics of Aluminum Combustion in Solid Rocket Propellants, *Proc. Combust. Inst.*, vol. **38**, no. 3, pp. 4417–4424, 2021.
- Melcher, J.C., Krier, H., and Burton, R.L., Burning Aluminum Particles inside a Laboratory-Scale Solid Rocket Motor, *J. Propuls. Power*, vol. **18**, no. 3, pp. 631–640, 2012.
- Sippel, T.R., Son, S.F., and Groven, L.J., Aluminum Agglomeration Reduction in a Composite Propellant Using Tailored Al/PTFE Particles, *Combust. Flame*, vol. **161**, no. 1, pp. 311–321, 2014.
- Sundaram, D.S., Puri, P., and Yang, V., A General Theory of Ignition and Combustion of Nano- and Micron-Sized Aluminum Particles, *Combust. Flame*, vol. **169**, pp. 94–109, 2016.
- Sundaram, D., Yang, V., and Yetter, R.A., Metal-Based Nanoenergetic Materials: Synthesis, Properties, and Applications, *Prog. Energy Combust. Sci.*, vol. **61**, pp. 293–365, 2017.
- Tu, C., Chen, X., Li, Y., Zhang, B., and Zhou, C., Experimental Study of Al Agglomeration on Solid Propellant Burning Surface and Condensed Combustion Products, *Def. Technol.*, vol. **26**, pp. 111–122, 2022.
- Wang, H., Jiang, Y., Wang, Y., Kline, D.J., Zheng, X., and Zachariah, M.R., Do We Need Perfect Mixing between Fuel and Oxidizer to Maximize the Energy Release Rate of Energetic Nanocomposites? *Appl. Phys. Lett.*, vol. **122**, no. 1, p. 011901, 2023a.
- Wang, H., Julien, B., Kline, D., Alibay, Z., Rehwoldt, M., Rossi, C., and Zachariah, M., Probing the Reaction Zone of Nanolaminates at $\sim \mu\text{s}$ Time and $\sim \mu\text{m}$ Spatial Resolution, *J. Phys. Chem. C*, vol. **124**, no. 25, pp. 13679–13687, 2020.
- Wang, H., Kline, D.J., Biswas, P., and Zachariah, M.R., Connecting Agglomeration and Burn Rate in a Thermite Reaction: Role of Oxidizer Morphology, *Combust. Flame*, vol. **231**, p. 111492, 2021a.
- Wang, H., Kline, D.J., Rehwoldt, M.C., and Zachariah, M.R., Carbon Fibers Enhance the Propagation of High Loading Nanothermites: In Situ Observation of Microscopic Combustion, *ACS Appl. Mater. Interfaces*, vol. **13**, no. 26, pp. 30504–30511, 2021b.
- Wang, H., Kline, D.J., Rehwoldt, M., Wu, T., Zhao, W., Wang, X., and Zachariah, M.R., Architecture Can Significantly Alter the Energy Release Rate from Nanocomposite Energetics, *ACS Appl. Polym. Mater.*, vol. **1**, no. 5, pp. 982–989, 2019a.
- Wang, H., Kline, D.J., and Zachariah, M.R., In-Operando High-Speed Microscopy and Thermometry of Reaction Propagation and Sintering in a Nanocomposite, *Nat. Commun.*, vol. **10**, no. 1, p. 3032, 2019b.
- Wang, H., Shen, J., Kline, D.J., Eckman, N., Agrawal, N.R., Wu, T., Wang, P., and Zachariah, M.R., Direct Writing of a 90 wt% Particle Loading Nanothermite, *Adv. Mater.*, vol. **31**, no. 23, p. 1806575, 2019c.
- Wang, H., Wang, Y., Garg, M., Moore, J.S., and Zachariah, M.R., Unzipping Polymers Significantly Enhance Energy Flux of Aluminized Composites, *Combust. Flame*, vol. **244**, p. 112242, 2022.
- Wang, Y., Hagen, E., Biswas, P., Wang, H., and Zachariah, M.R., Imaging the Combustion Characteristics of Al, B, and Ti Composites, *Combust. Flame*, vol. **252**, p. 112747, 2023b.

